

Supporting Information

Light-Triggered Dual-Modality Drug Release of Self-Assembled Prodrug-Nanoparticles for Synergistic Photodynamic and Hypoxia-Activated Therapy

Dongyang Zhao,^a Wenhui Tao,^a Songhao Li,^a Lingxiao Li,^a Yixin Sun,^a Guanting Li,^a Gang Wang,^b Yang Wang,^b Bin Lin,^c Cong Luo,^a Yongjun Wang,^a Maosheng Cheng,^c Zhonggui He^{*a} and Jin Sun^{*a}

^a Department of Pharmaceutics, Wuya College of Innovation, Shenyang Pharmaceutical University, Shenyang 110016, China.

E-mail: hezhonggui@vip.163.com; sunjin@syphu.edu.cn

^b College of Pharmacy, Guangxi University of Chinese Medicine, Nanning 530200, China

^c Key Laboratory of Structure-Based Drug Design and Discovery, Shenyang Pharmaceutical University, Shenyang 110016, China

Experimental Section

Materials: Pyropheophorbide a (PPa) was purchased from Shanghai Xianhui Pharmaceutical Co., Ltd (Shanghai, China). Mercaptoacetic acid, LiAlH_4 , 1,6-hexandiol, 4-dimethylaminopyridine (DMAP), triphosgene, N-methylmorpholine (NMM), and H_2O_2 were purchased from Aladdin Co., Ltd (Shanghai, China). p-Toluenesulfonic acid (TsOH), 2-(7-azabenzotriazol-1-yl)-N, N, N', N'-tetramethyluronium hexafluorophosphate (HATU), and 1,3-diphenylisobenzofuran (DPBF) were purchased from J&K Scientific Co., Ltd (Beijing, China). 2,2'-thiodiethanol was purchased from Huaxia Reagent Co., Ltd (Chengdu, China). 1,2-distearoylsn-glycero-3-phosphoethanolamine-N-[methoxy(polyethyleneglycol)-2000] (DSPE-PEG_{2k}) was obtained from Shanghai Advanced Vehicle Technology Co., Ltd (Shanghai, China). Fluorometric thiol quantitation kit was purchased from Sigma-Aldrich Corp., (St. Louis, MO, USA). Cell culture reagents were obtained from GIBCO, Invitrogen Corp. (Carlsbad, California, USA). Cell culture dish/plate and 20 mm glass-bottom dish were obtained from NEST Biotechnology Co., Ltd (Wuxi, China). Hoechst 33342 was obtained from BD Biosciences (New Jersey, USA). MTT, trypsin-EDTA, and Bouin's fluid were purchased from Dalian Meilun Biotechnology Co., Ltd (Dalian, China). Hypoxia/oxidative stress detection kit was purchased from Enzo Life Sciences, Inc. (Farmingdale, USA). All other reagents and solvents mentioned in this article were of analytical grade.

Synthesis and Characterization of TKOH: Mercaptoacetic acid (1.38 g, 15 mmol) and catalytic amounts of TsOH (2.5 mg, 15 μmol) in anhydrous acetone (2.2 mL, 30 mmol) were stirred at room temperature. After stirring for 6 h, the reaction was stopped and the flask was placed in an ice-salt mixture. The precipitated crystals were then filtered, washed with hexane and ice-cold water. After drying in vacuum, TKCOOH was obtained as a white solid. Then TKCOOH (1.12 g, 5 mmol) in anhydrous THF (10 mL) was dropwise added to LiAlH_4 (0.759 g, 20 mmol) in anhydrous THF (15 mL) under stirring and the mixture was refluxed for 8 h. Then the reaction mixture was slowly added 10% NaOH aqueous solution in an ice bath under stirring until no

gas was generated. After filtering, the filtrate was dried over anhydrous Na₂SO₄. The solution was concentrated by a rotatory evaporator, and the crude product was purified by silica column chromatography to obtain TKOH as colorless oil in a yield of 92.5%. The product was confirmed by Bruker AV-400 NMR Spectroscopy (Bruker, Germany). ¹H NMR (600 MHz, DMSO-d₆, δ): 4.81 (t, *J* = 5.6 Hz, 2H), 3.52 (td, *J* = 7.0, 5.5 Hz, 4H), 2.65 (t, *J* = 7.1 Hz, 4H), 1.52 (s, 6H).

Synthesis and Characterization of PR104A: PR104A was synthesized and the product was confirmed by SolariX 7.0T ESI-MS (Bruker, Germany) and Bruker AV-400 NMR Spectroscopy (Bruker, Germany). HRMS (ESI) *m/z*: [M – H][–] calcd for C₁₄H₁₈BrN₄O₉S, 496.99834; found, 496.99865. ¹H NMR (400 MHz, CDCl₃, δ): 8.63 (d, *J* = 2.8 Hz, 1H), 8.59 (d, *J* = 2.8 Hz, 1H), 4.40 (t, *J* = 5.1 Hz, 2H), 3.88 (t, *J* = 5.0 Hz, 2H), 3.70 – 3.63 (m, 4H), 3.62 – 3.53 (m, 4H), 3.01 (s, 3H).

Synthesis and Characterization of PR104A-S-OH, PR104A-TK-OH, and PR104A-OH: DMAP (58.88 mg, 0.48 mmol) in anhydrous DCM (2 mL) was dropwise added to a mixture solution of PR104A (100 mg, 0.2 mmol) and triphosgene (20.88 mg, 0.07 mmol) in anhydrous DCM (50 mL) at approximately 0 °C under stirring. After stirring for 1 h, 2,2'-thiodiethanol (245.35 mg, 2 mmol), TKOH (393.55 mg, 2 mmol), or 1,6-hexandiol (237.3 mg, 2 mmol) in anhydrous DCM (2 mL) was added, and the reaction mixture was stirred overnight at room temperature. The mixture was washed with 1 N HCl aqueous solution (2 × 50 mL) and a saturated NaCl solution (2 × 50 mL). The organic layer was separated and dried over anhydrous Na₂SO₄. The solution was concentrated by a rotatory evaporator, and the crude product was purified by preparative liquid chromatography to obtain PR104A-S-OH, PR104A-TK-OH, or PR104A-OH as a yellow gum in a yield of 35.5%, 45.2%, or 42.6%, respectively. The products were confirmed by SolariX 7.0T ESI-MS (Bruker, Germany) and Bruker AV-400 NMR Spectroscopy (Bruker, Germany).

HRMS (ESI) m/z : $[M - H]^-$ calcd for $C_{19}H_{26}BrN_4O_{12}S_2$, 645.01775; found, 645.01763. 1H NMR (400 MHz, $CDCl_3$, δ): 8.63 (d, $J = 2.7$ Hz, 1H), 8.57 (d, $J = 2.8$ Hz, 1H), 7.40 (s, 1H), 4.46 – 4.37 (m, 4H), 4.34 (t, $J = 6.3$ Hz, 2H), 3.78 (q, $J = 5.2$ Hz, 2H), 3.74 (t, $J = 5.8$ Hz, 2H), 3.67 – 3.53 (m, 6H), 3.01 (s, 3H), 2.84 (t, $J = 6.4$ Hz, 2H), 2.76 (t, $J = 5.9$ Hz, 2H).

HRMS (ESI) m/z : $[M - H]^-$ calcd for $C_{22}H_{32}BrN_4O_{12}S_3$, 719.03677; found, 719.03844. 1H NMR (400 MHz, $CDCl_3$, δ): 8.63 (d, $J = 2.7$ Hz, 1H), 8.56 (d, $J = 2.8$ Hz, 1H), 7.52 (s, 1H), 4.40 (t, $J = 4.8$ Hz, 4H), 4.35 (t, $J = 6.5$ Hz, 2H), 3.80 – 3.72 (m, 4H), 3.66 – 3.52 (m, 6H), 3.01 (s, 3H), 2.96 (t, $J = 6.6$ Hz, 2H), 2.82 (t, $J = 6.2$ Hz, 2H), 1.61 (s, 6H).

HRMS (ESI) m/z : $[M - H]^-$ calcd for $C_{21}H_{30}BrN_4O_{12}S$, 641.07698; found, 641.07662. 1H NMR (400 MHz, $CDCl_3$, δ): 8.63 (d, $J = 2.8$ Hz, 1H), 8.56 (d, $J = 2.8$ Hz, 1H), 7.36 (s, 1H), 4.39 (t, $J = 5.0$ Hz, 4H), 4.18 (t, $J = 6.6$ Hz, 2H), 3.78 (q, $J = 5.3$ Hz, 2H), 3.65 – 3.55 (m, 8H), 3.01 (s, 3H), 1.74 – 1.66 (m, 2H), 1.41 (p, $J = 3.5$ Hz, 4H), 1.31 – 1.23 (m, 2H).

Synthesis and Characterization of PR104A-S-PPa, PR104A-TK-PPa, and PR104A-PPa:

HATU (92.4 mg, 0.24 mmol) in anhydrous acetonitrile (2 mL) was dropwise added to a mixture solution of PPa (100 mg, 0.19 mmol) and NMM (51.6 μ L, 0.47 mmol) in anhydrous DCM (50 mL) at approximately 0 °C under stirring. After stirring for 1 h, PR104A-S-OH (121 mg, 0.19 mmol), PR104A-TK-OH (134.8 mg, 0.19 mmol), or PR104A-OH (120.2 mg, 0.19 mmol) in anhydrous DCM (2 mL) was added, and the reaction mixture was stirred overnight at room temperature. The mixture was washed with 1 N HCl aqueous solution (2×50 mL) and a saturated NaCl solution (2×50 mL). The organic layer was separated and dried over anhydrous Na_2SO_4 . The solution was concentrated by a rotatory evaporator, and the crude product was purified by preparative liquid chromatography to obtain PR104A-S-PPa, PR104A-TK-PPa, or PR104A-PPa as a black solid in a yield of 75.3%, 78.5%, or 75.5%, respectively. The products were confirmed by SolariX 7.0T ESI-MS (Bruker, Germany) and Bruker AV-400 NMR Spectroscopy (Bruker, Germany).

HRMS (ESI) m/z : $[M + H]^+$ calcd for $C_{52}H_{60}BrN_8O_{14}S_2$, 1163.28483; found, 1163.28363.

1H NMR (400 MHz, $CDCl_3$, δ): 9.48 (s, 1H), 9.37 (s, 1H), 8.59 (s, 1H), 8.52 (d, $J = 2.8$ Hz, 1H), 8.47 (d, $J = 2.8$ Hz, 1H), 7.99 (dd, $J = 17.8, 11.6$ Hz, 1H), 7.42 (t, $J = 5.9$ Hz, 1H), 6.33 – 6.15 (m, 2H), 5.26 (d, $J = 19.8$ Hz, 1H), 5.09 (d, $J = 19.8$ Hz, 1H), 4.55 – 4.43 (m, 1H), 4.35 – 4.30 (m, 1H), 4.26 (q, $J = 5.0$ Hz, 4H), 4.21 (t, $J = 6.5$ Hz, 2H), 4.15 – 4.08 (m, 2H), 3.70 – 3.60 (m, 7H), 3.50 (t, $J = 6.2$ Hz, 2H), 3.44 (t, $J = 5.9$ Hz, 4H), 3.41 (s, 3H), 3.22 (s, 3H), 2.91 (s, 3H), 2.77 – 2.65 (m, 3H), 2.64 – 2.52 (m, 3H), 2.38 – 2.25 (m, 2H), 1.83 (d, $J = 7.2$ Hz, 3H), 1.67 (t, $J = 7.6$ Hz, 3H), 0.36 (s, 1H), –1.72 (s, 1H).

HRMS (ESI) m/z : $[M + H]^+$ calcd for $C_{55}H_{66}BrN_8O_{14}S_3$, 1237.30385; found, 1237.30869.

1H NMR (400 MHz, $CDCl_3$, δ): 9.45 (s, 1H), 9.34 (s, 1H), 8.58 (s, 1H), 8.53 (d, $J = 2.8$ Hz, 1H), 8.47 (d, $J = 2.8$ Hz, 1H), 7.98 (dd, $J = 17.8, 11.6$ Hz, 1H), 7.36 (t, $J = 5.9$ Hz, 1H), 6.33 – 6.13 (m, 2H), 5.26 (d, $J = 21.0$ Hz, 1H), 5.10 (d, $J = 19.8$ Hz, 1H), 4.55 – 4.44 (m, 1H), 4.34 – 4.29 (m, 1H), 4.26 (q, $J = 4.5$ Hz, 4H), 4.22 (t, $J = 6.7$ Hz, 2H), 4.18 – 4.09 (m, 2H), 3.68 – 3.59 (m, 7H), 3.55 – 3.48 (m, 2H), 3.48 – 3.42 (m, 4H), 3.41 (s, 3H), 3.20 (s, 3H), 2.92 (s, 3H), 2.82 (t, $J = 6.7$ Hz, 2H), 2.72 (t, $J = 6.8$ Hz, 2H), 2.70 – 2.63 (m, 1H), 2.62 – 2.52 (m, 1H), 2.39 – 2.23 (m, 2H), 1.83 (d, $J = 7.2$ Hz, 3H), 1.67 (t, $J = 7.6$ Hz, 3H), 1.51 (d, $J = 5.4$ Hz, 6H), 0.36 (s, 1H), –1.74 (s, 1H).

HRMS (ESI) m/z : $[M + H]^+$ calcd for $C_{54}H_{64}BrN_8O_{14}S$, 1159.34406; found, 1159.34726.

1H NMR (400 MHz, $CDCl_3$, δ): 9.46 (s, 1H), 9.35 (s, 1H), 8.58 (s, 1H), 8.55 (d, $J = 2.8$ Hz, 1H), 8.49 (d, $J = 2.8$ Hz, 1H), 7.98 (dd, $J = 17.8, 11.6$ Hz, 1H), 7.32 (t, $J = 5.8$ Hz, 1H), 6.31 – 6.13 (m, 2H), 5.25 (d, $J = 19.8$ Hz, 1H), 5.09 (d, $J = 19.8$ Hz, 1H), 4.56 – 4.45 (m, 1H), 4.33 – 4.25 (m, 5H), 4.08 (t, $J = 6.6$ Hz, 2H), 4.01 – 3.93 (m, 2H), 3.70 – 3.61 (m, 7H), 3.57 – 3.51 (m, 2H), 3.50 – 3.44 (m, 4H), 3.40 (s, 3H), 3.20 (s, 3H), 2.92 (s, 3H), 2.75 – 2.63 (m, 1H), 2.60 – 2.50 (m, 1H), 2.39 – 2.21 (m, 2H), 1.83 (d, $J = 7.3$ Hz, 3H), 1.67 (t, $J = 7.6$ Hz, 3H), 1.52 – 1.43 (m, 2H), 1.26 – 1.14 (m, 4H), 0.95 – 0.79 (m, 2H), 0.36 (s, 1H), –1.74 (s, 1H).

Preparation and Characterization of Prodrug-NPs: Heterodimeric prodrugs (PR104A-S-PPa, PR104A-TK-PPa, or PR104A-PPa) (4 mg) and DSPE-PEG_{2k} (0.8 mg) were dissolved in acetone (1 mL) and then added dropwise into deionized water (4 mL) under stirring (1000 rpm). Self-assembly of prodrug-NPs occurred spontaneously. Acetone in the nano-formulation was then evaporated under vacuum, and the organic solvent-free prodrug-NPs were stored at 4 °C. The particle size, polydispersity index (PDI), and zeta potential of prodrug-NPs were measured by Nano ZS Zetasizer instrument (Malvern, UK). The morphology of prodrug-NPs was observed using JEM-2100 transmission electron microscope (JEOL, Japan).

Colloidal Stability of Prodrug-NPs: Prodrug-NPs with a final concentration of 0.25 mg mL⁻¹ were incubated in pH 7.4 PBS supplemented with 10% of FBS for 24 h at 37 °C, and particle size was measured at pre-determined time intervals (0, 2, 4, 6, 8, 10, 12, and 24 h). In addition, prodrug-NPs with a final concentration of 1 mg mL⁻¹ were stored at 4 °C for 2 weeks to investigate the long-term stability.

In Vitro Drug Release from Prodrug-NPs: PSP NPs, PTKP NPs, or PP NPs (100 µg equivalent PR104A) were incubated in 30 mL pH 7.4 PBS release media in the presence of 10 mM H₂O₂ at 37 °C or under 660 nm laser irradiation (100 mW cm⁻²) (n = 3). At the pre-determined time points, the concentration of the released PR104A and the remaining prodrugs were determined by high performance liquid chromatography (HPLC).

To investigate the light-triggered drug release mechanism, the molecular weight of prodrugs was measured by micrOTOF-Q ESI-MS (Bruker, Germany) after 660 nm laser irradiation (100 mW cm⁻²) for 5 min. In addition, fluorometric thiol quantitation kit was used to monitor the thiol generation after prodrug-NPs or prodrug-NPs added with excess vitamin C as ROS scavenger receiving 660 nm laser irradiation (100 mW cm⁻²) at different time points (n = 3).

In Vitro ¹O₂ Detection and O₂ Consumption: DPBF in DMSO (6 µL, 5 mM) was added to aqueous solutions (3 mL) of free PPa, PSP NPs, PTKP NPs, or PP NPs (20 µg mL⁻¹ equivalent

PPa). The absorption spectrum of the mixtures under 660 nm laser irradiation (100 mW cm⁻²) was obtained on a UV-1102 II UV-Vis spectrophotometer (Techcomp, China) every 1 min. Meanwhile, the dissolved O₂ in the above mixtures was also measured using a JPB-607A portable dissolved oxygen meter (INESA, China) at the end of the ¹O₂ detection assay.

Cell Culture: 4T1 mouse breast cancer cells were originally purchased from the American Type Culture Collection (ATCC) and cultured in Gibco RPMI-1640 medium supplemented with 10% FBS, penicillin (100 U mL⁻¹) and streptomycin (100 µg mL⁻¹). The cells were maintained in a humidified atmosphere of 5% CO₂ at 37 °C.

Cellular Uptake: 4T1 cells were seeded in 12-well plates at a density of 1 × 10⁵ cells per well and incubated for 24 h. Then, cells were washed and incubated with free PPa solution, PSP NPs, PTKP NPs, or PP NPs (2 µg mL⁻¹ equivalent PPa) for 4 h at 37 °C. After incubation, cells were washed and fixed with 4% paraformaldehyde for 10 min at room temperature. Then, the cells were washed again, and the nuclei were counterstained by Hoechst for 10 min. The prepared covered slips were examined by TCS SP2/AOBS confocal laser scanning microscopy (CLSM) (LEICA, Germany).

For flow cytometry analysis, cells were washed, harvested, and suspended in PBS after incubation with different formulations. Untreated cells were utilized as control. Intracellular fluorescence intensity was measured by FACSCalibur flow cytometer (BD, USA).

In addition, after incubation with formulations for 4 h, cells were washed, harvested, and suspended in PBS. Then, the cells were broken by ultrasonication, and the supernatants were obtained after protein precipitation. More precise cellular uptake was investigated by determination of the cellular concentration of PPa or prodrugs using HPLC (n = 3).

Intracellular ROS/Hypoxia Detection: 4T1 cells were seeded in 20 mm glass-bottom dishes at a density of 5 × 10⁴ cells per dish and incubated for 24 h. Then, cells were washed and incubated with PSP NPs, PTKP NPs, or PP NPs (2 µg mL⁻¹ equivalent PPa) for 4 h at 37 °C. After

incubation, cells were washed and treated with hypoxia/oxidative stress detection kit according to the manufacturer's instructions. After 30 min, the cells were washed and exposed to 660 nm laser irradiation (100 mW cm^{-2}) for 1 min. After irradiation, cells were washed and observed by TCS SP2/AOBS confocal laser scanning microscopy (CLSM) (LEICA, Germany).

For flow cytometry analysis, after irradiation, cells were washed, collected, and suspended in PBS. Intracellular fluorescence intensity was measured by FACSCalibur flow cytometer (BD, USA). The dyes were excited with an excitation wavelength of 488 nm and detected in the FL3 channel (hypoxia) and FL1 channel (oxidative stress), respectively. The negative and positive (ROS-induced and hypoxia-induced) control samples were also included in the experiment for 4T1 cells.

Intracellular Drug Release from Prodrug-NPs: 4T1 cells were seeded in 12-well plates at a density of 1×10^5 cells per well and incubated for 24 h. Then, cells were washed and incubated with PSP NPs, PTKP NPs, or PP NPs ($2 \mu\text{g mL}^{-1}$ equivalent PPa) for 4 h at $37 \text{ }^\circ\text{C}$ ($n = 3$). After incubation, cells were washed and irradiated with 660 nm laser (100 mW cm^{-2}) for 5 min. The cells together with the drug-containing PBS were collected, and the cells were broken by ultrasonication. The concentrations of free PR104A in the solutions were determined by HPLC.

Cytotoxicity Assay: 4T1 cells were seeded in 96-well plates at a density of 1000 cells per well and incubated for 24 h. Then, cells were treated with serial dilutions of free PPa solution, PR104A & PPa mixture, PSP NPs, PTKP NPs, or PP NPs. After incubation for 4 h, the laser-treated groups received 660 nm laser irradiation (100 mW cm^{-2}) for 5 min and further incubated for 20 h. Subsequently, $20 \mu\text{L}$ of the MTT solution (5 mg mL^{-1}) was added into the wells. After incubation for 4 h, the medium was replaced with DMSO ($150 \mu\text{L}$). The absorbance was measured with a wavelength of 570 nm by the microplate reader (BioTek, USA). The cytotoxicity of free PR104A against 4T1 cells in hypoxia and normoxia conditions was also evaluated. The hypoxia environment was simulated by pre-incubated cells with $100 \mu\text{M CoCl}_2$.

Animal Studies: Male Sprague-Dawley rats and female BALB/c mice were obtained from the Laboratory Animal Center of Shenyang Pharmaceutical University. All the animal experiments were carried out according to the Guidelines for the Care and Use of Laboratory Animals approved by the Institutional Animal Ethical Care Committee (IAEC) of Shenyang Pharmaceutical University.

In Vivo Pharmacokinetic Study: Male Sprague-Dawley rats (220–250 g) were intravenously administrated with free PR104A solution, PSP NPs, PTKP NPs, or PP NPs at a dose of 2.8 mg kg⁻¹ equivalent to PR104A (n = 3). Blood samples were collected into heparin tubes at 0.083, 0.5, 1, 2, 4, 6, 8, 12, and 24 h after intravenous injection. The blood samples were centrifuged to obtain plasma, and the plasma samples were stored at –80 °C until analysis. The plasma concentrations of prodrugs and PR104A were measured by HPLC. In addition, the *in vitro* plasma stability of prodrug-NPs was also evaluated by incubation with rat plasma at 37 °C. At prescriptive intervals, 100 µL samples were withdrawn and 200 µL acetonitrile was added. After vortex and centrifugation, the concentrations of prodrugs in the supernatants were determined by HPLC.

In Vivo Biodistribution: 4T1 cells (5×10^5) were injected into the mammary fat pad of female BALB/c mice. When the tumor reached 200–250 mm³, mice were intravenously administrated with free PPa solution, PSP NPs, PTKP NPs, or PP NPs at a dose of 3 mg kg⁻¹ equivalent to PPa (n = 3). At 4, 12, 24, and 36 h after intravenous injection, mice were anesthetized and imaged using IVIS® Lumina III Small Animal Imaging System (PerkinElmer, USA). The mice were sacrificed at 36 h post-injection, the organs including heart, liver, spleen, lung, kidney, and tumor were collected and subjected to *ex vivo* fluorescence imaging. In addition, the obtained tumors were homogenized, more precise tumor accumulation was investigated by determination of the concentration of PPa or prodrugs using HPLC (n = 3).

In Vivo Antitumor Efficacy: 4T1 cells (5×10^6) or 4T1 cells (5×10^5) were inoculated subcutaneously or injected into the mammary fat pad of female BALB/c mice to establish

heterotopic or orthotopic 4T1 tumor-bearing mice models, respectively. When the tumor size was around 100 mm³, mice were intravenously administrated with saline, free PR104A solution, free PPa solution, PR104A & PPa mixture, PSP NPs, PTKP NPs, or PP NPs at a dose of 2.8 mg kg⁻¹ equivalent to PR104A and 3 mg kg⁻¹ equivalent to PPa at days 0, 2, 4, and 6 (n = 5). The laser-treated groups received 660 nm laser irradiation (200 mW cm⁻²) for 5 min at 24 h post-injection. Body weight and tumor growth of the mice were recorded at days 0, 2, 4, 6, 8, 10, and 12. The tumor growth was monitored by digital caliper, and the volumes calculated as tumor volume (mm³) = 0.5 × length × width². On day 12, the mice were sacrificed, the tumors were weighed, and the blood samples were centrifuged to obtain the serums for hepatorenal function analysis. Tumor and major organs of mice were histopathologically analyzed via hematoxylin and eosin (H&E) staining. The lungs of orthotopic 4T1 tumor-bearing mice were fixed in Bouin's solution for 18 h, and stored in 70% ethanol. The surface tumors in pulmonary lobes were counted and recorded.

Statistical Analysis: Data were presented as mean ± SD. Comparison between groups was analyzed with Student's t-test and one-way analysis of variance (ANOVA), and statistical differences were considered significant at p < 0.05.

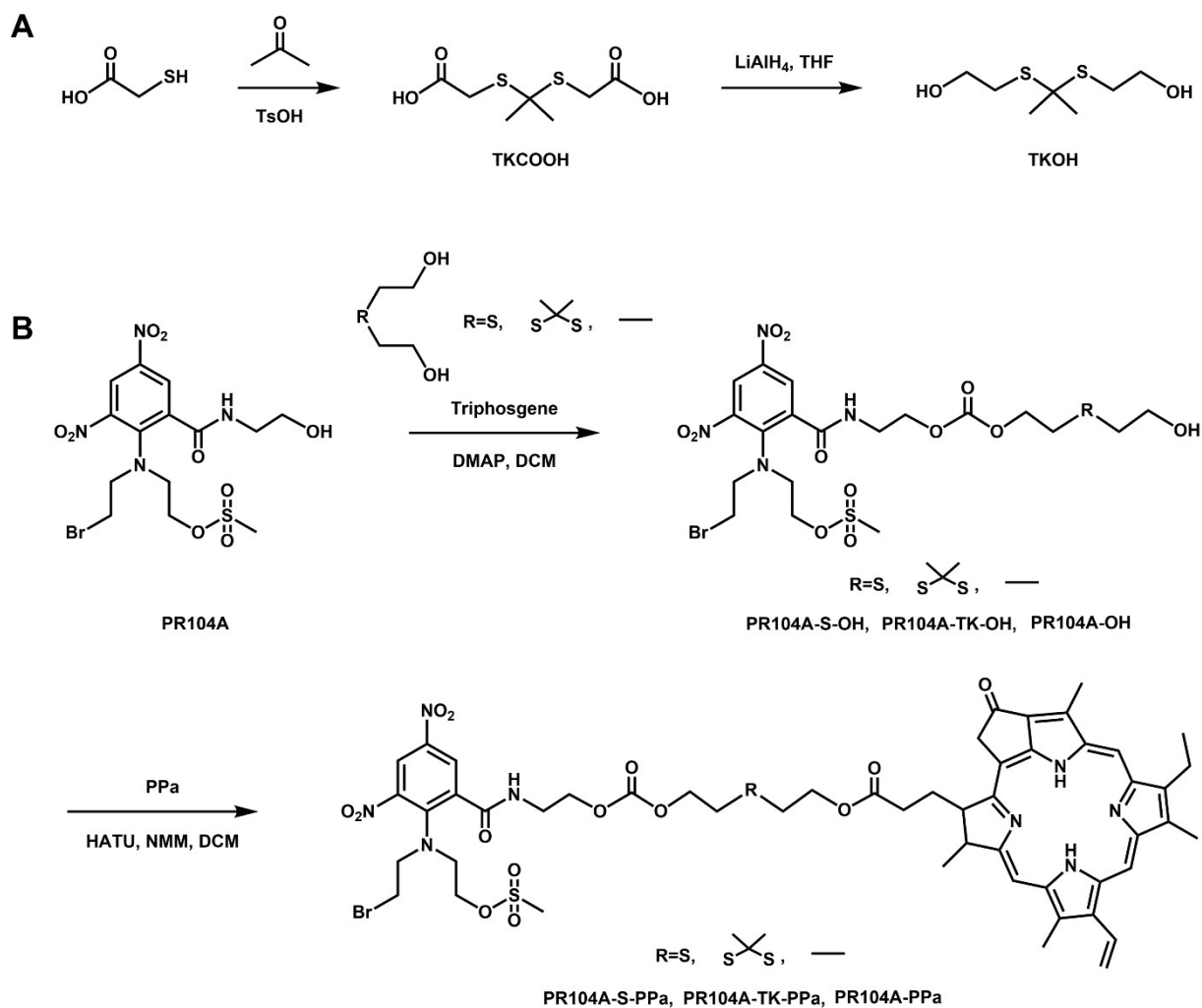


Fig. S1. The synthetic routes of (A) TKOH, (B) PR104A-S-OH, PR104A-TK-OH, PR104A-OH, PR104A-S-PPa, PR104A-TK-PPa, and PR104A-PPa.

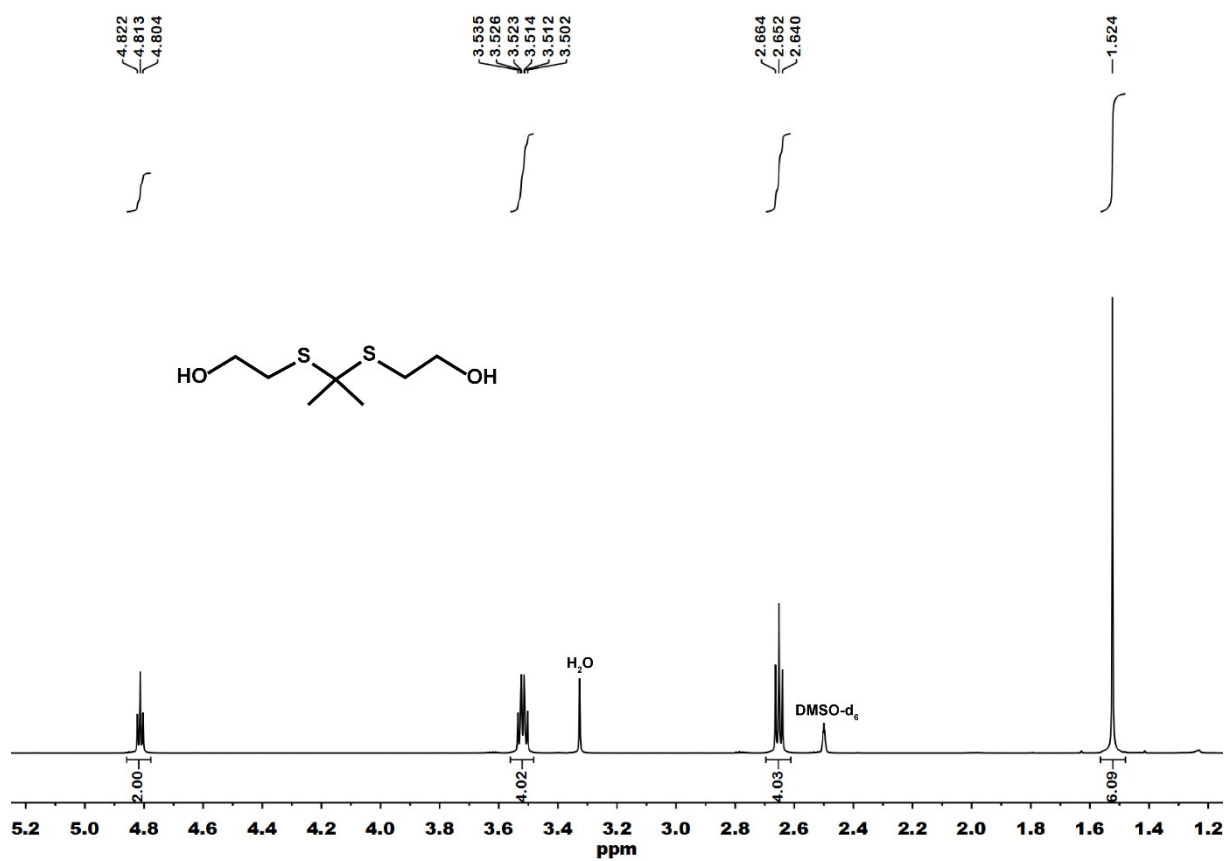


Fig. S2. ^1H NMR (600 MHz, DMSO-d_6) of TKOH.

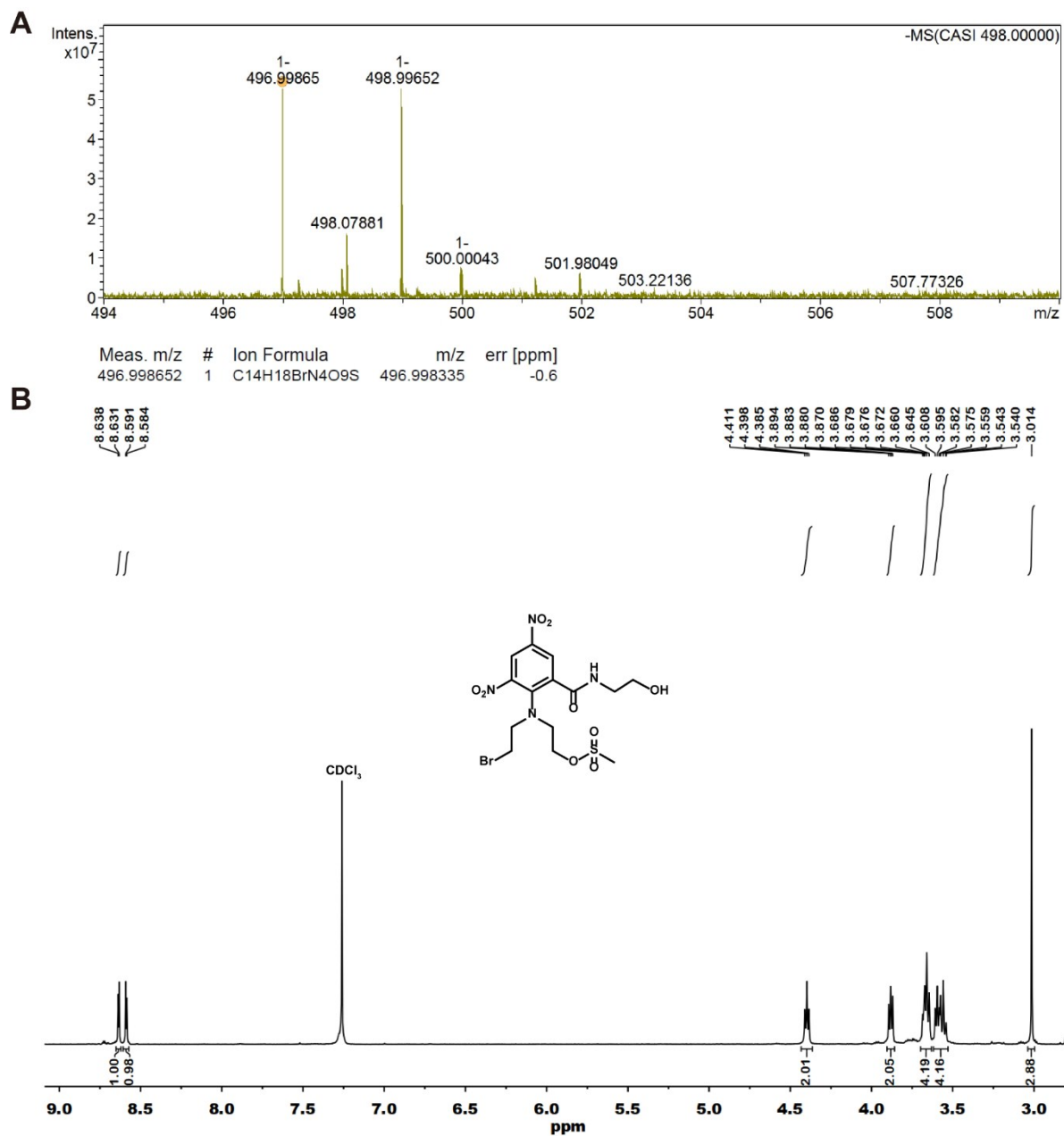


Fig. S3. (A) ESI-MS and (B) ¹H NMR (400 MHz, CDCl₃) of PR104A.

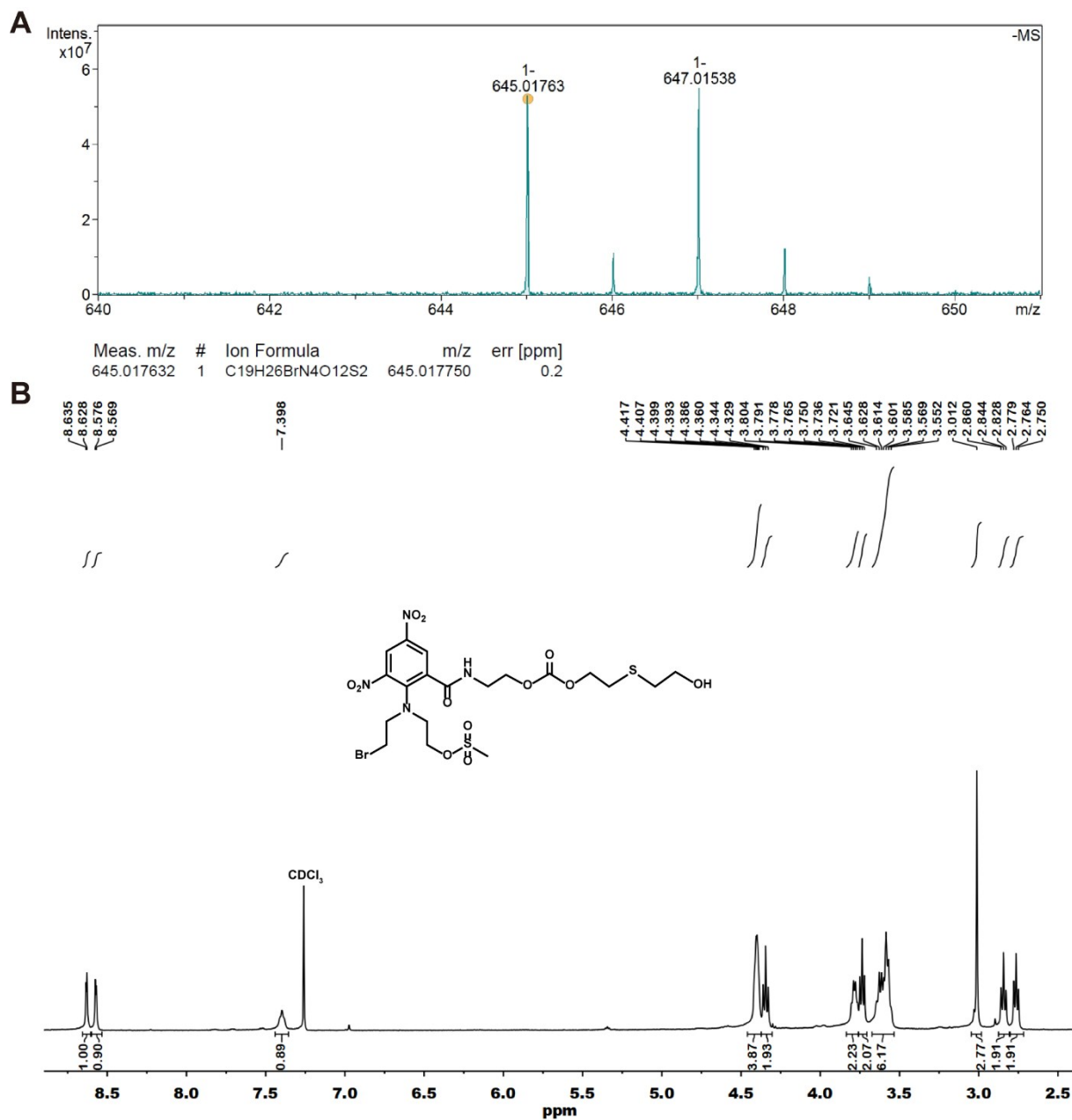


Fig. S4. (A) ESI-MS and (B) ¹H NMR (400 MHz, CDCl₃) of PR104A-S-OH.

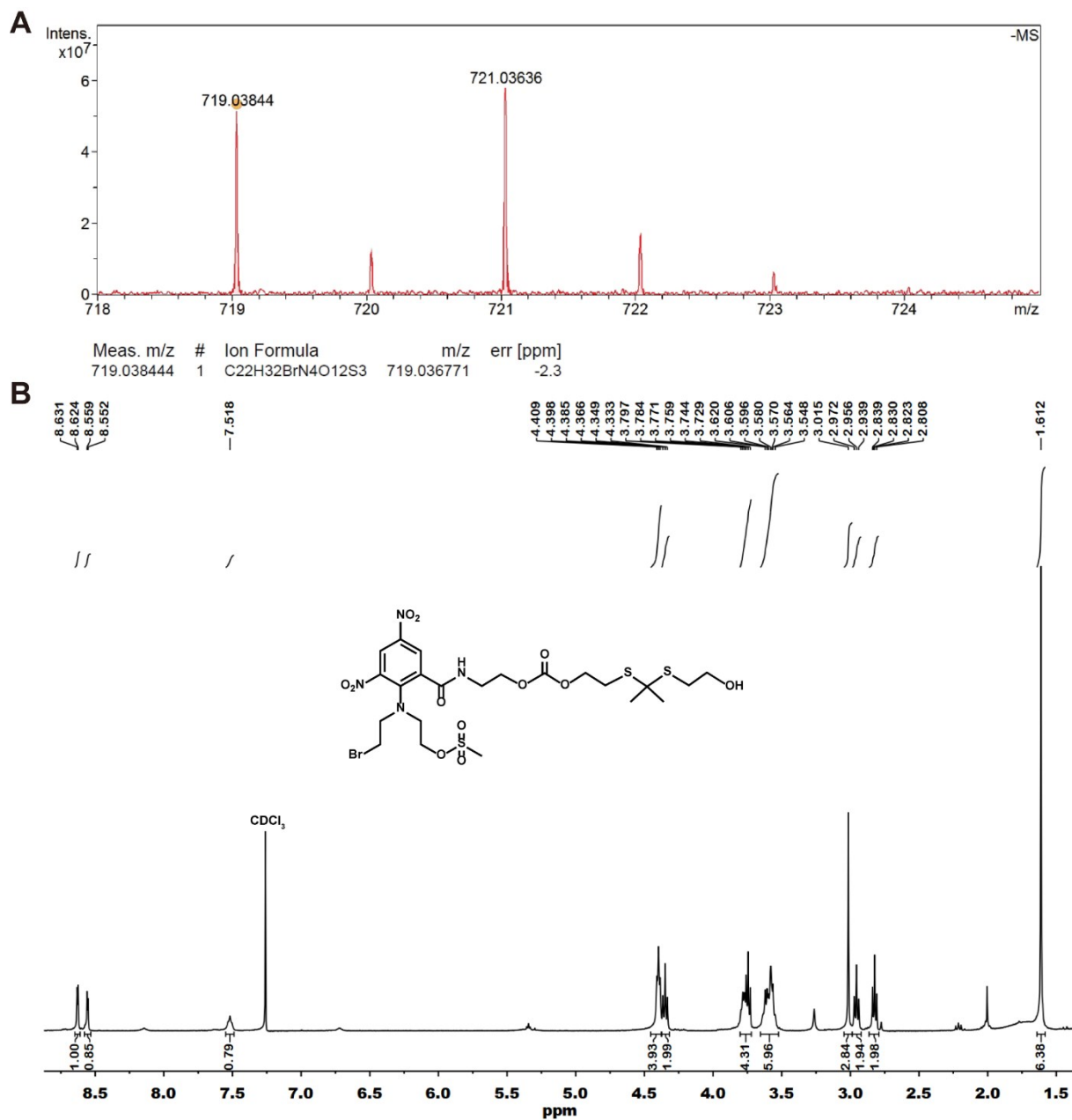


Fig. S5. (A) ESI-MS and (B) ^1H NMR (400 MHz, CDCl_3) of PR104A-TK-OH.

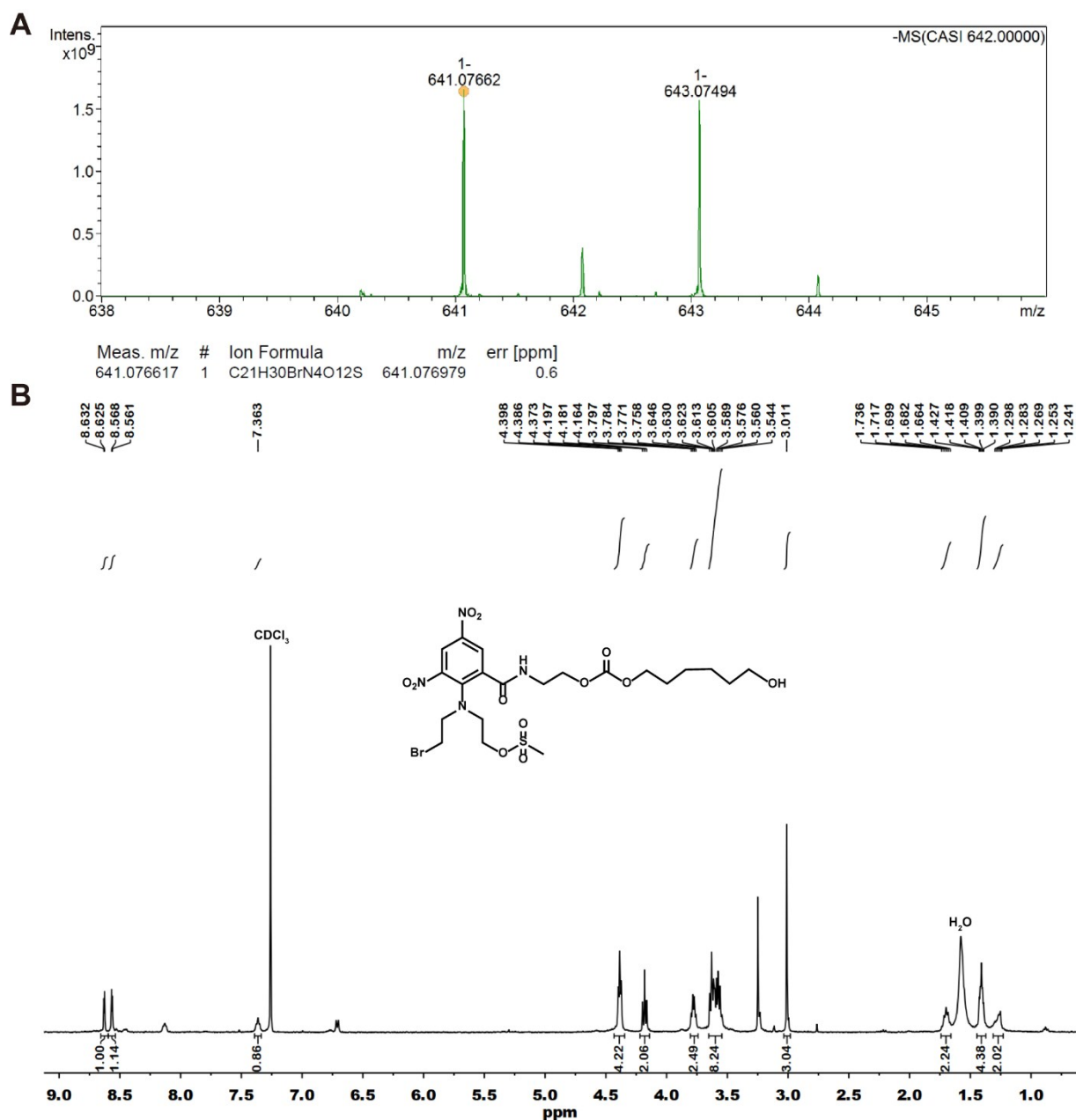


Fig. S6. (A) ESI-MS and (B) ¹H NMR (400 MHz, CDCl₃) of PR104A-OH.

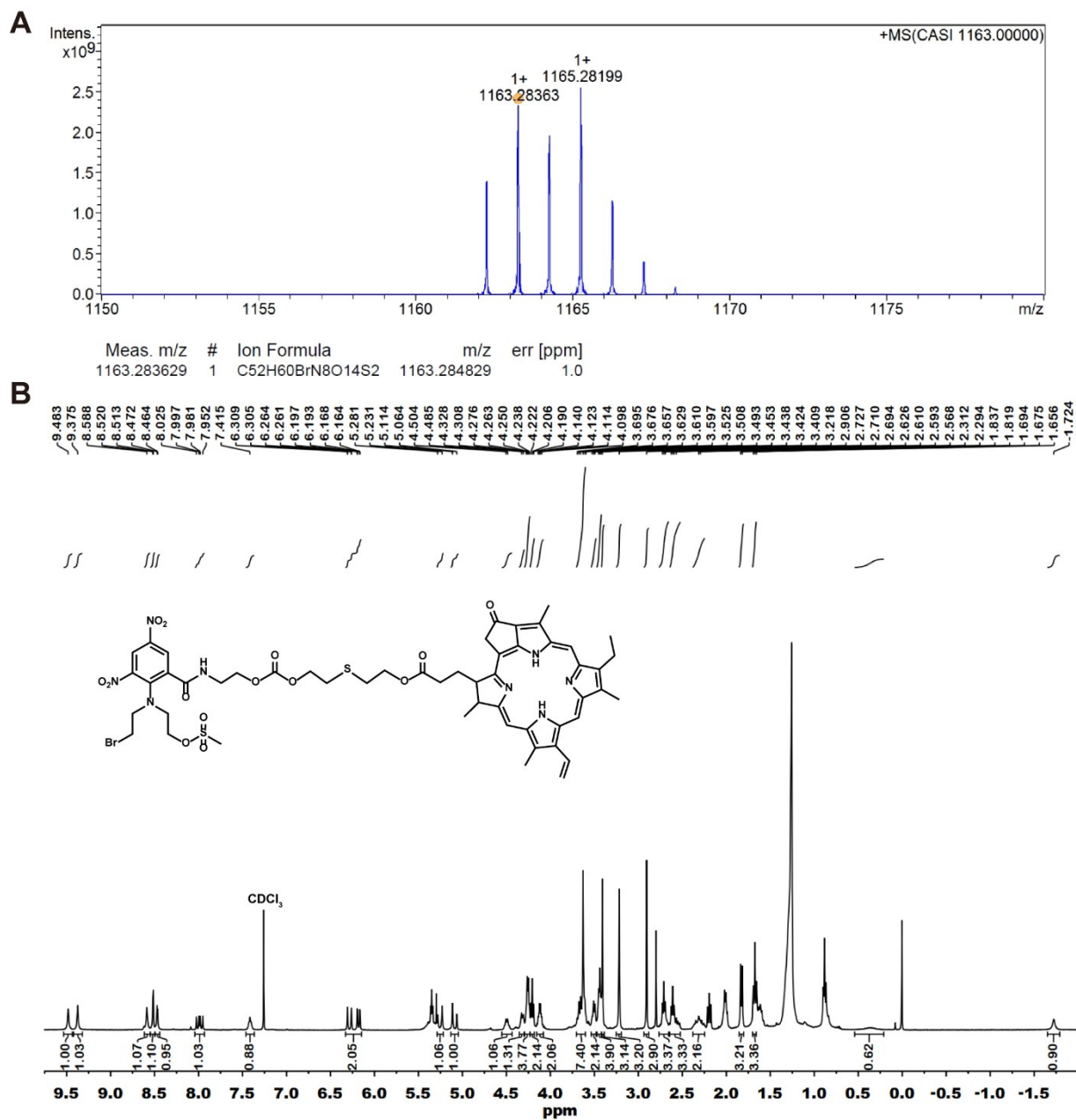


Fig. S7. (A) ESI-MS and (B) ¹H NMR (400 MHz, CDCl₃) of PR104A-S-PPa.

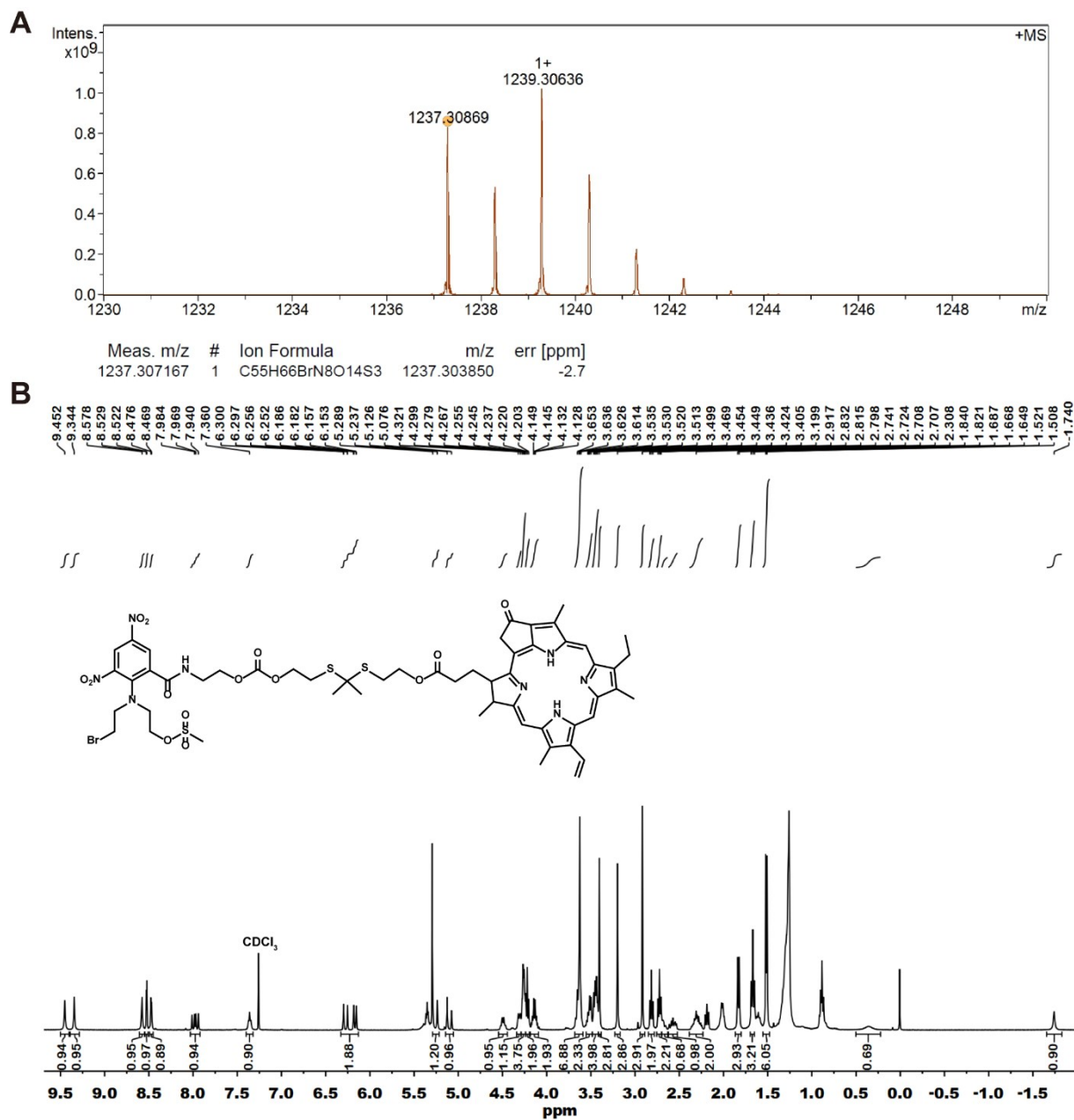


Fig. S8. (A) ESI-MS and (B) ¹H NMR (400 MHz, CDCl₃) of PR104A-TK-PPa.

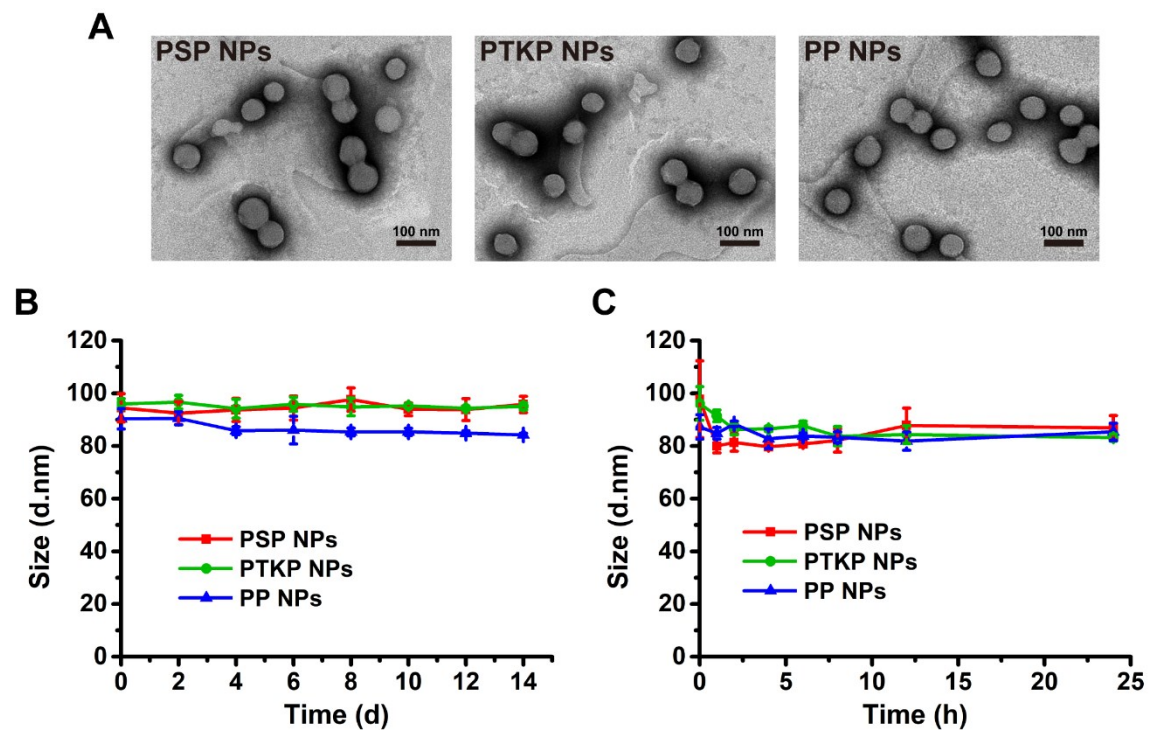


Fig. S10. (A) TEM images of prodrug-NPs. Stability of prodrug-NPs (B) after storage at 4 °C for 2 weeks and (C) after incubation in PBS (pH 7.4) supplemented with 10% FBS at 37 °C for 24 h.

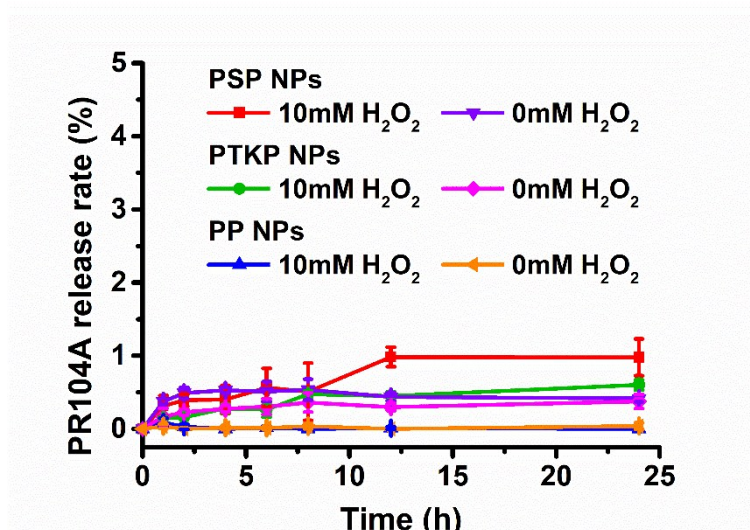


Fig. S11. *In vitro* PR104A release of prodrug-NPs in the presence of 10 mM H₂O₂ (n = 3).

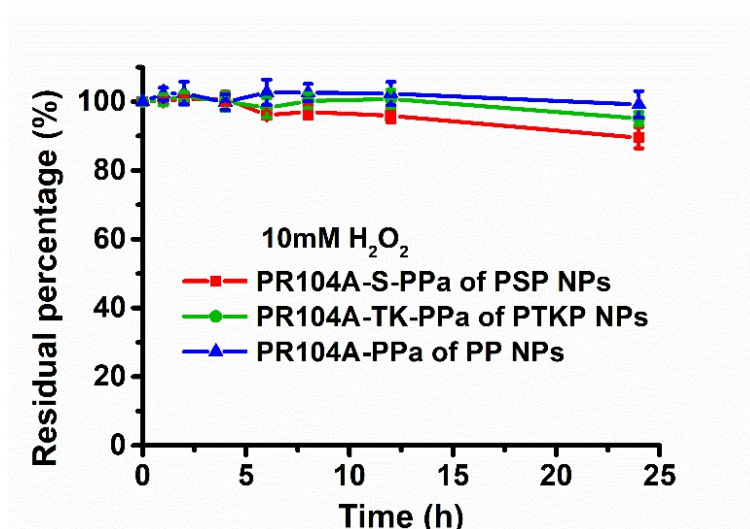


Fig. S12. Residual percentage of PR104A-S-PPa, PR104A-TK-PPa, and PR104A-PPa after PSP NPs, PTKP NPs, and PP NPs were treated with 10 mM H₂O₂, respectively (n = 3).

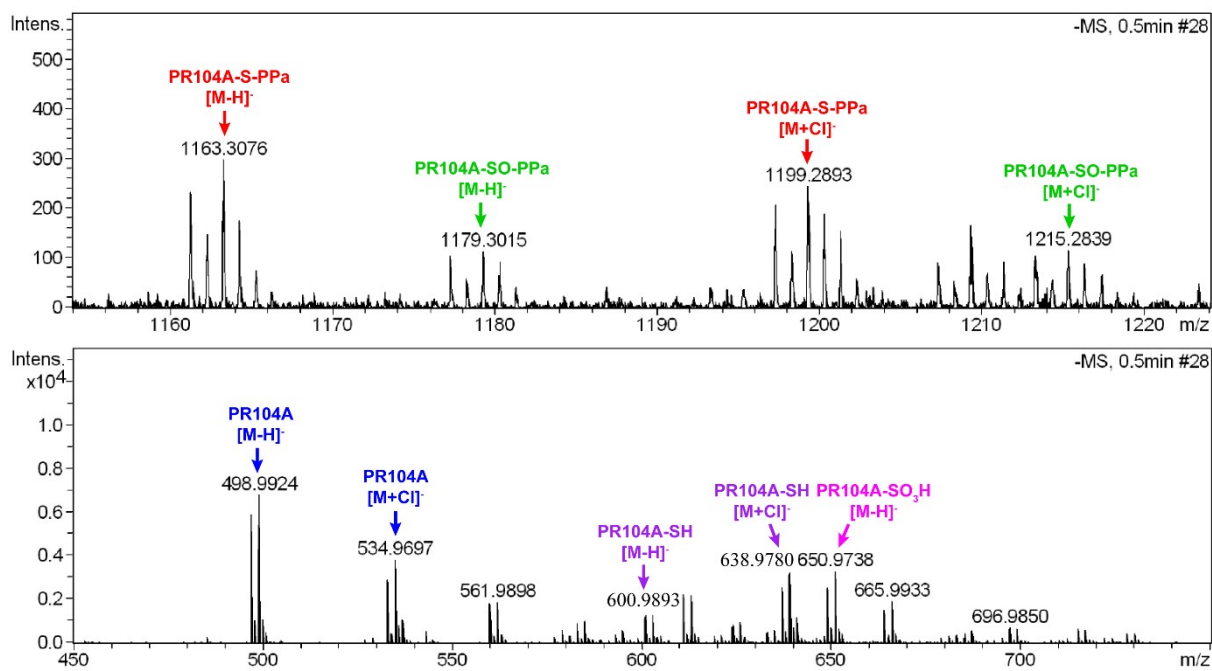


Fig. S13. ESI-MS of PSP NPs after 660 nm laser irradiation (100 mW cm^{-2}) for 5 min.

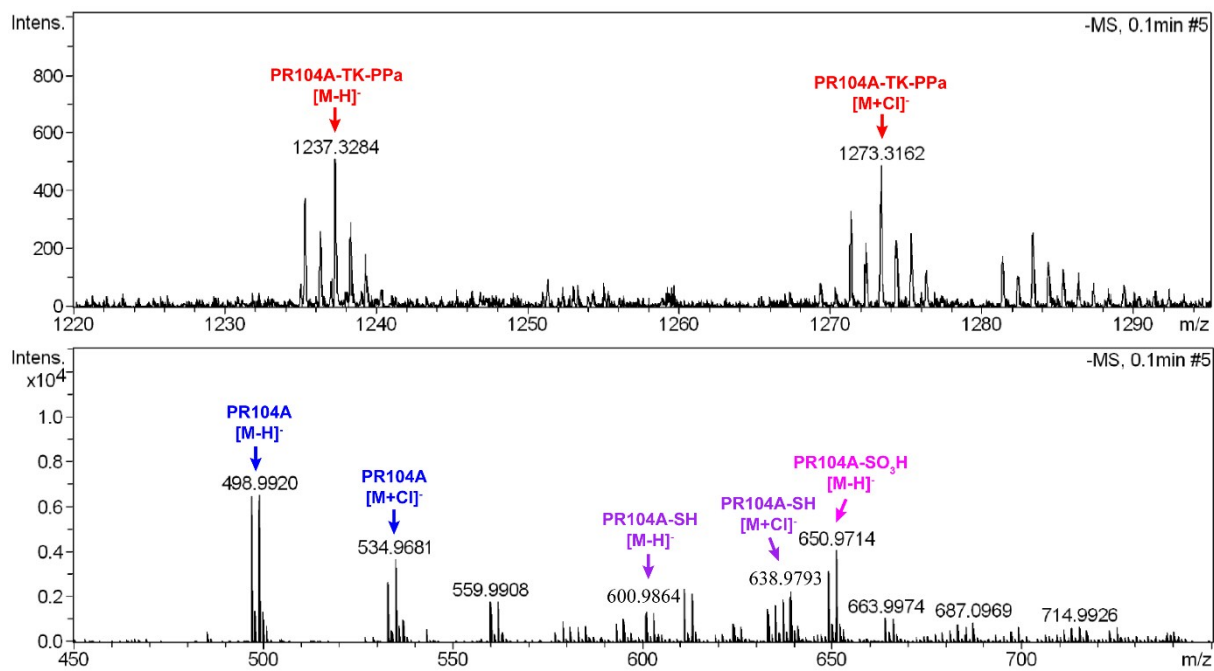


Fig. S14. ESI-MS of PTKP NPs after 660 nm laser irradiation (100 mW cm^{-2}) for 5 min.

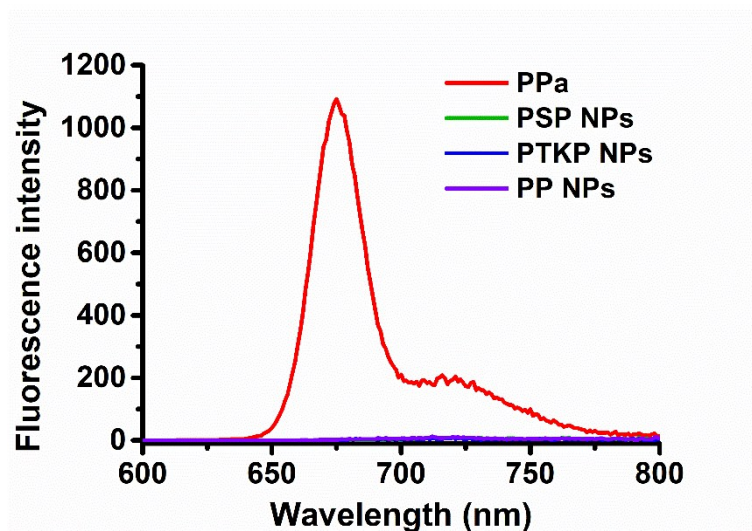


Fig. S15. Fluorescence spectrum of free PPa and prodrug-NPs ($1 \mu\text{g mL}^{-1}$, PPa equivalent).

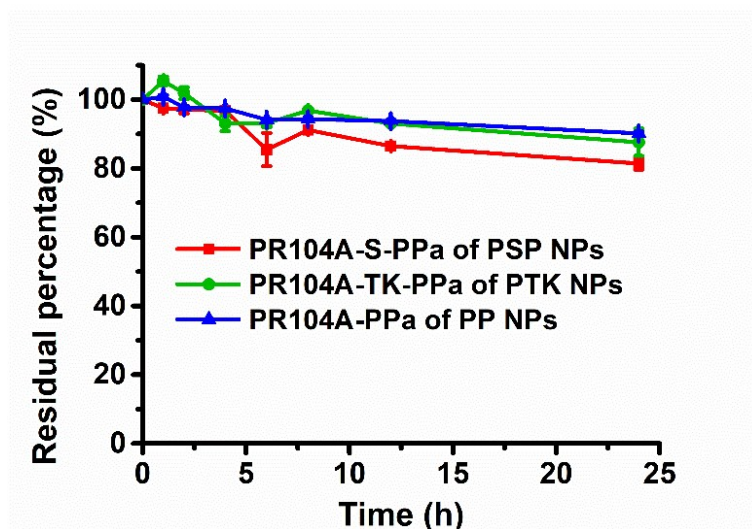


Fig. S16. Residual percentage of PR104A-S-PPa, PR104A-TK-PPa, and PR104A-PPa of prodrug-NPs after incubation with rat plasma at 37 °C (n = 3).

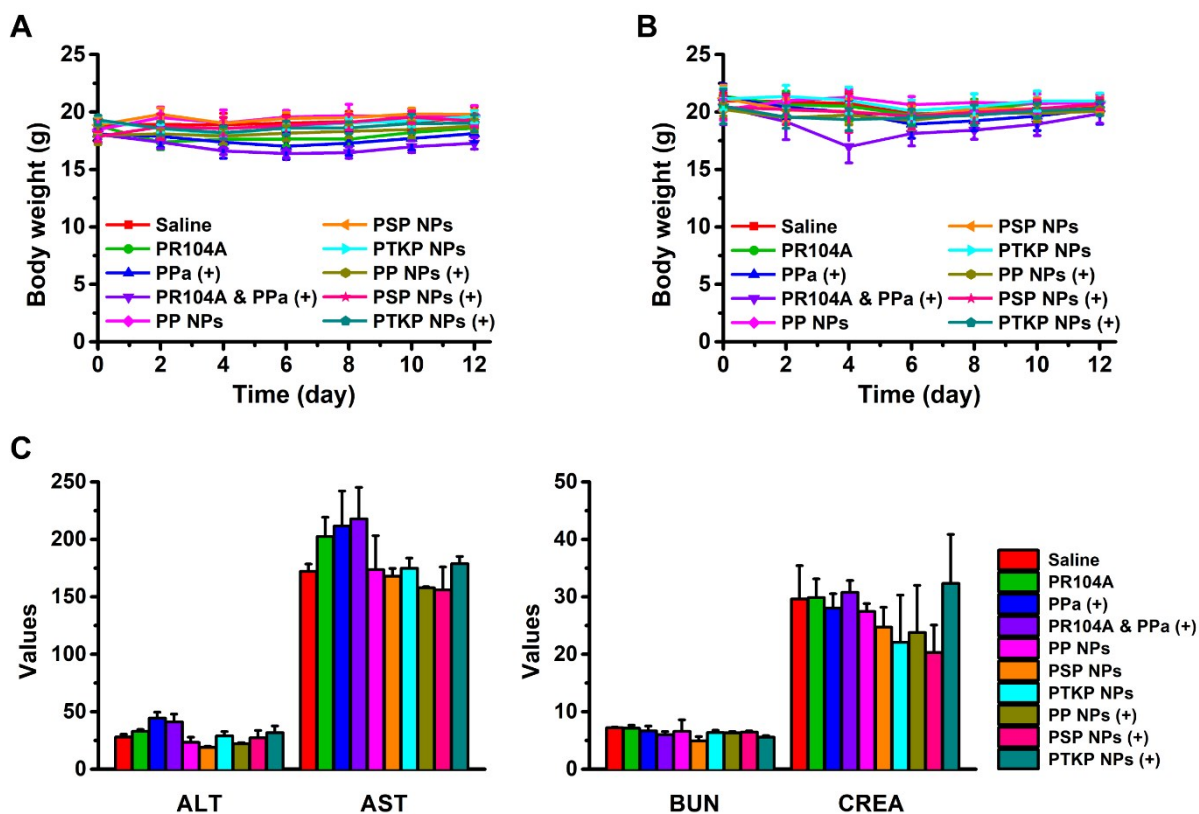


Fig. S17. Body weight changes of (A) heterotopic and (B) orthotopic 4T1 tumor-bearing mice after i.v. administration with different formulations ($n = 5$). (C) Hepatorenal function parameters of orthotopic 4T1 tumor-bearing mice after treatments ($n = 3$). ALT (U L^{-1}): alanine aminotransferase; AST (U L^{-1}): aspartate aminotransferase; BUN (mmol L^{-1}): blood urea nitrogen; CREA ($\mu\text{mol L}^{-1}$): creatinine. (+): laser irradiation.

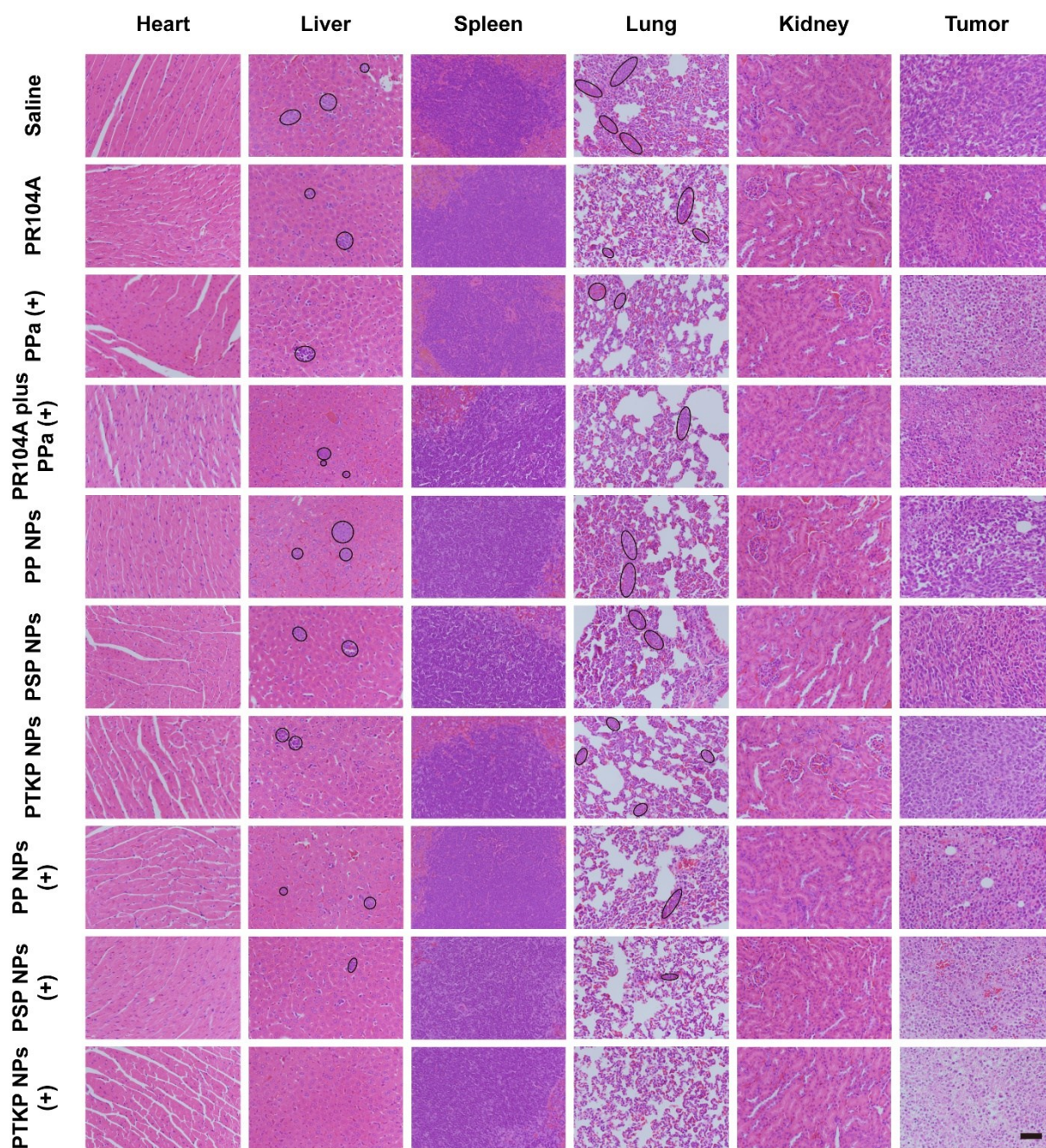


Fig. S18. H&E staining of the major organs of orthotopic 4T1 tumor-bearing mice after different treatments. Scale bar represents 100 μ m. Black circles denote surface lung and liver metastases. (+): laser irradiation.

Table S1. Characteristics of prodrug-nanoassemblies (n = 3).

Nanoassemblies	Size [d.nm] ^{a)}	PDI ^{a)}	Zeta potential [mV] ^{a)}	PR104A drug loading [%] ^{b)}	PPa drug loading [%] ^{b)}
PSP NPs	99.0 ± 4.4	0.16 ± 0.03	-31.7 ± 1.4	35.7%	38.3%
PTKP NPs	97.5 ± 2.5	0.18 ± 0.04	-31.1 ± 3.6	33.6%	36.0%
PP NPs	87.6 ± 1.3	0.11 ± 0.01	-29.2 ± 3.0	35.8%	38.4%

^{a)} Mean diameters, polydispersity index, and zeta potential of nanoassemblies were determined by DLS; ^{b)} Drug loading of PR104A or PPa was calculated by the molecular weight of conjugates and the amount of DSPE-PEG_{2k}.

Table S2. Cytotoxicity (IC₅₀ values) of different formulations against 4T1 cell line. (+): laser irradiation.

Formulations	IC ₅₀ (μM)
PR104A (normoxia)	> 80
PR104A (hypoxia)	> 10
PPa (+)	0.1381
PR104A & PPa (+)	0.0885
PSP NPs	> 40
PTKP NPs	> 40
PP NPs	> 100
PSP NPs (+)	0.3245
PTKP NPs (+)	0.2382
PP NPs (+)	0.8564

Table S3. Pharmacokinetic parameters of PR104A, PSP NPs, PTKP NPs, and PP NPs (n = 3).

Formulations	Determined ^a	AUC _{0-24h} [h nmol mL ⁻¹] ^b	t _{1/2} [h] ^c
PR104A	PR104A	1.03 ± 0.19	0.30 ± 0.19
PSP NPs	PR104A-S-PPa	331.13 ± 15.90	1.84 ± 0.12
	PR104A	0.42 ± 0.09	0.88 ± 0.02
PTKP NPs	PR104A-TK-PPa	386.06 ± 35.12	2.10 ± 1.21
	PR104A	0.22 ± 0.04	0.59 ± 0.02
PP NPs	PR104A-PPa	422.76 ± 17.02	1.50 ± 0.24
	PR104A	0.09 ± 0.09	2.19 0.79

^a) Prodrugs and the released PR104A were simultaneously determined; ^b) Area under the plasma concentration-time curve; ^c) Half-life.